Carbohydrate Polymers 94 (2013) 301–308

Contents lists available at SciVerse ScienceDirect

Carbohydrate Polymers

journal homepage: www.elsevier.com/locate/carbpol

Stimulation of lymphocyte proliferation by oyster glycogen sulfated at C-6 position

Jingfeng Yang[a,b], Beiwei Zhu[a,b,*], Jie Zheng[c], Liming Sun[b], Dayong Zhou[b], Xiuping Dong[b], Chenxu Yu[d]

[a] School of Food and Biological Engineering, Jiangsu University, Zhenjiang 212013, PR China
[b] School of Food Science and Technology, Dalian Polytechnic University, Dalian 116034, PR China
[c] Liaoning Ocean and Fisheries Science Research Institute, Dalian 116023, PR China
[d] Department of Agricultural and Biosystems Engineering, Iowa State University, Ames, IA 50011, USA

ARTICLE INFO

Article history:
Received 1 September 2012
Received in revised form 19 January 2013
Accepted 21 January 2013
Available online 28 January 2013

Keywords:
Oyster
Glycogen
Polysaccharide
Sulfation
Structure–activity correlation
Lymphocyte proliferation

ABSTRACT

In this study, glycogen was extracted from oyster *Ostrea talienwhanensis* Crosse and used as a model to investigate the structure–activity correlation of polysaccharides. Purified oyster glycogen was characterized by methylation analysis, nuclear magnetic resonance (NMR) spectroscopy and infrared spectroscopy (IR). The oyster glycogen was subsequently sulfated by chlorosulfonic acid–pyridine method, and a C-6 substituted species (SOG) was identified to be the primary sulfated oyster glycogen species by ^{13}C NMR spectroscopy. The molecular weight and sulfate content of the SOG was determined to be 3.2×10^4 g/mol and 33.6%, respectively. Another sulfated oyster glycogen species (SOG1) with C-2 and C-3 substitution was also identified at a lesser amount in the final product. SOG exhibited a much stronger stimulation effect to splenic lymphocyte proliferation than SOG1 *in vitro*, indicating that the position of sulfate substitution is a major determining factor on the efficacy of sulfated glycogens to stimulate lymphocyte proliferation.

1. Introduction

Sulfated polysaccharides have been found to exhibit various biological activities such as antivirus, antitumor, anticoagulant and lymphocyte proliferation stimulation (Sudipta et al., 2012; Sun et al., 2009; Wijesinghe, Athukorala, & Jeon, 2011; Ye, Xu, & Li, 2012) that rely on the molecular weight and sulfate content (Yoshiaki et al., 1987). However, the huge structural diversity of these macromolecules, e.g. the differences in monosaccharide composition, glycosidic linkages, position and distribution of substituents, and various three-dimensional structures and isomeric forms, has rendered it difficult to establish precise structure–activity correlations for these molecules (Ghosh et al., 2009). Nevertheless, some evidence suggested that the position of sulfate substituent is important for the bioactivity. For example, changing the position of sulfate substituent from 4-*O*-sulphated to 6-*O*-sulphated in galactosamine leads to almost complete disappearance of anticoagulant activity, in spite of high overall level of sulfation (Mulloy, Mourão, & Gray, 2000).

Although the bioactivity of some polysaccharides has been known for decades, the lack of comprehensive structural information has limited the effort to study their potential for clinical use (Dourado et al., 2004). The oyster *Ostrea talienwhanensis* Crosse glycogen is a uniform glucose polymer, consisting mainly of α-(1→4) glucose linkage with high branches at C-6 positions. The oyster glycogen is an ideal model for the investigation of polysaccharide structure–activity correlation because of its simple composition and linkage structure. In this study, the purified oyster glycogen was sulfated at the C-6 position specifically to reveal the structure–activity correlation.

2. Materials and methods

2.1. Materials

Oysters, *O. talienwhanensis* Crosse were purchased from Dalian Changxing aquatic products market, China. They were all collected from the Yellow Sea, China. After manually removing the shells, the oysters were thoroughly washed with tap water, freeze-dried, and smashed for subsequent glycogen extraction.

Pepsin and papain were purchased from Sangon Biotechnology Co. (Shanghai, China). Bovine serum albumin (BSA) and DEAE-cellulose-52 were obtained from Fluka Chemie Co. (Buchs, Switzerland) and GE Healthcare Co. (USA), respectively.

* Corresponding author at: School of Food Science and Technology, Dalian Polytechnic University, No. 1 Qinggongyuan, Ganjingzi District, Dalian 116034, PR China. Tel.: +86 411 86323262; fax: +86 411 86323262.
E-mail address: zhubeiwei@163.com (B. Zhu).

0144-8617/$ – see front matter © 2013 Elsevier Ltd. All rights reserved.
http://dx.doi.org/10.1016/j.carbpol.2013.01.057

Monosaccharide standards and Sephadex G-100 were obtained from Pharmacia Co. (Uppsala, Sweden). MD-25 dialysis tubes (MWCO: 7 kg/mol) were purchased from Amersham Co. (Uppsala, Sweden). All chemicals used in this study were of analytical grade or above.

2.2. Experimental methods

Total sugar content was measured by phenol–sulfuric acid method using glucose as standard (Dubois, Gilles, Hamilton, Rebers, & Smith, 1956). Protein content was determined as described by Bradford (1976) using BSA as standard. Sulfate content was assessed after hydrolyzing the glycogen samples with 1 M HCl using potassium sulfate as standard (Therho & Hartiala, 1971). IR spectroscopic measurement was conducted with Specord 75 IR spectrometer (Carl Zeiss, Jena). All chromatographic assays were conducted with phenol–sulfuric acid method.

2.3. Sample preparation of oyster polysaccharide

Because of the high protein content, the oyster samples were deproteinized first as follows: the smashed freeze-dried oyster samples were dissolved into distilled water at 1:45 (w/v) and hydrolyzed by pepsin for 2 h at pH 2.0 (37 °C). After cooling, the solution was adjusted to pH 7.0 and centrifuged at 4000 × *g* for 10 min. The supernatant was collected and concentrated under reduced pressure. Threefold volume of 95% ethanol (v/v) was then added into the enzymatic hydrolysate under constant stirring and incubated overnight. Subsequently the solution was centrifuged at 4000 × *g* for 10 min. The precipitate was washed twice with absolute ethanol to yield the crude oyster polysaccharide. The entire procedure was then repeated with the enzyme being replaced by papain at pH 6.0 to remove the conjugate proteins. The dissociative proteins were then removed using Sevag method (Staub, 1965).

The crude oyster polysaccharide was further purified by a series of column chromatographic separation procedures. Firstly, the crude sample was loaded onto a diethylaminoethyl anion exchange column (DEAE-cellulose-52, 2.0 cm × 40 cm) equilibrated with 0.15 M NaCl. The elution procedure was performed orderly with distilled water, 0.15 M NaCl and 0.5 M NaCl at a flow rate of 24 mL/h. The fractions with major polysaccharide contents were combined and further purified by a Sephadex G-100 column (1.6 cm × 70 cm) equilibrated with 0.15 M NaCl. The eluent was 0.15 M NaCl, and the flow rate was 24 mL/h. The major fraction was then collected, concentrated, desalted by dialysis and then vaccum freeze-dried to obtain the homogeneous polysaccharide.

2.4. Structural characterization of oyster polysaccharide

2.4.1. Monosaccharide compositional analysis

The monosaccharide composition of oyster polysaccharide was evaluated through quantitative analysis of its 1-phenyl-3-methyl-5-pyrazolone (PMP) derivatives using liquid chromatography. 2 mg of the oyster polysaccharide was dissolved in 1 mL trifluoroacetic acid (TFA, 2 M), and was subsequently hydrolyzed at 121 °C for 2 h. The hydrolysate was fully converted to PMP derivatives by this process (Strydom, 1994). The monosaccharide composition was then characterized using a Shimadzu liquid chromatography system (LC-10Avp Plus) with a Tigerkin C_{18} column (4.6 mm × 250 mm, 5 μm). The injection amount of the sample solution was 20 μL, and the elution was performed with a mixture of PBS (Na_2HPO_4–NaH_2PO_4, 0.1 M, pH 6.7) and acetonitrile (83:17, v/v) at a flow rate of 1 mL/min. Monosaccharide standards were converted to their PMP derivatives following identical protocol and used as references for the characterization of unknown monosaccharides from samples. The amount of monosaccharides was determined quantitatively by measuring the peak areas calibrated with the monosaccharide standards.

2.4.2. Methylation analysis

The oyster polysaccharide was methylated according to the method of Needs and Selvendran (1993). The completion of methylation was indicated by the disappearance of hydroxyl absorption peak in IR spectrum at 3400 cm^{-1}. The methylated products were depolymerized with 85% formic acid for 4 h (100 °C) and then further hydrolyzed with 2 M TFA for 6 h at the same temperature. The hydrolysate was then reduced and acetylated. The products were quantitatively analyzed by GC–MS method described by Yang, Zhou, and Liang (2009), and the exact types of methylated alditol acetates and their molar ratios were obtained.

2.4.3. Nuclear magnetic resonance (NMR) spectroscopic analysis

The polysaccharide samples (30 mg) were ultrasonically (30 min) dissolved in deuteroxide, and then they were subjected to NMR analysis (Bruker AV-500). The spectrometer was operated at 500.13 MHz (^1H) and 125.75 MHz (^{13}C).

2.5. Sulfation of oyster glycogen

The sulfation of oyster glycogen was conducted using the chlorosulfonic acid/pyridine method (Lu, Wang, Hu, Huang, & Wang, 2008). Briefly, 2 g glycogen and 40 mL anhydrous formanide were thoroughly mixed and then 60 mL of sulphation reagent (a mixture of chlorosulfonic acid and pyridine with mole ratio 1:5) was added. The mixture was kept at 60 °C for 3 h, and then it was blended into 100 mL ice water and adjusted to pH 7.0 with 20% NaOH. After precipitation with 95% ethanol, the precipitate was re-dissolved and dialyzed against distilled water. The experiment was repeated three times and the products from each run were combined and loaded onto a DEAE-cellulose-52 column (Pharmacia Co., Sweden) for separation. Substance recovered from the main peak was concentrated, desalted by dialysis and lyophilized to yield the final sulfated oyster glycogen product. FT-IR was conducted to confirm the sulfation reaction results.

2.6. Homogeneity analysis and molecular weight determination

The homogeneity of sulfated and unsulfated oyster glycogen samples was determined by a Shimadzu liquid chromatography system (LC-10Avp Plus) with a TSK-gel G4000PWXL column (7.8 mm × 300 mm, TOSOH, Japan) and a 2000ES evaporative light scattering detector (ELSD). 20 μL of sample solution (2 mg/mL) was injected into the liquid chromatography system for each run, and eluted with distilled water at a flow rate of 0.2 mL/min. The molecular weight of samples were determined by a column of Sephorose CL-6B (1.2 cm × 60 cm), eluted with 0.15 M NaCl. The column was calibrated by standard Dextrans (4.1×10^5 g/mol, 2.7×10^5 g/mol, 8×10^4 g/mol, 1.2×10^4 g/mol, Sigma).

2.7. Assay of lymphocyte proliferation activity

Spleens were aseptically extirpated from 3 Kunming species mice. Spleen cells were obtained according to Sun et al. (2010). The splenocyte density was adjusted to 5×10^6 cells per mL. Cell viability was more than 98% as determined by trypan blue staining method.

The proliferation of spleen lymphocyte was determined using MTT assay (Mosmann, 1983). An aliquot of 100 μL of the splenocytes was seeded into 96-well microplate, and then the original glycogen and the sulfated glycogen at different concentrations (10,

Table 1
Methylation analysis and NMR spectrum signals assigned of the purified glycogen from oyster *Ostrea talienwhanensis* Crosse.

Linkage pattern	Methylation analysis		Chemical shifts (δ)					
	Methylated product	Molar ratio	C1/H1	C2/H2	C3/H3	C4/H4	C5/H5	C6/H6
α-D-Glc*p*(1→	1,5-Ac_2-2,3,4,6-Me_4-Glc*p*	1	100.5/5.40	71.9/3.84	73.4/3.72	70.1/3.44	73.6/3.68	61.2/3.86, 3.78
→4)-α-D-Glc*p*(1→	1,4,5-Ac_3-2,3,6-Me_3-Glc*p*	8.103	100.5/5.40	72.3/3.63	74.1/3.99	77.6/3.66	71.9/3.84	61.2/3.86, 3.78
→4,6)-α-D-Glc*p*(1→	1,4,5,6-Ac_4-2,3-Me_2-Glc*p*	1.224	100.5/5.40	72.5/3.60	73.4/3.72	77.6/3.66	70.1/3.44	–
→6)-α-D-Glc*p* (1→	1,5,6-Ac_3-2,3,4-Me_3-Glc*p*	0.082	–	–	–	–	–	–
→2,4)-α-D-Glc*p* (1→	1,2,4,5-Ac_4-3,6-Me_2-Glc*p*	0.096	–	–	–	–	–	–
→3)-α-D-Glc*p* (1→	1,3,5-Ac_3-2,4,6-Me_3-Glc*p*	0.022	–	–	–	–	–	–

–, no signal.

20, 40, 50 and 100 μg/mL) were added. After incubation at 37 °C for 44 h, 20 μL MTT solution (5 mg/mL) was added into each well. The cells were further incubated for an additional 4 h, and then an aliquot of 100 μL DMSO was added to the cell culture and homogenized for 15 min to fully dissolve the formazan product. The absorbance at 450 nm was measured on an ELISA reader (Model 680, Bio-Rad, USA) to benchmark the proliferation activity. All measurements were conducted in quintuple.

3. Results and discussion

3.1. Preparation of the oyster polysaccharide

The chemical composition of oyster samples was measured as sugar content 33.17%, protein content 38.78%, lipid content 17.72% and water content 2.67%. Polysaccharide was extracted from oyster *O. talienwhanensis* Crosse by enzymolysis with pepsin. The extraction yield was calculated as 25.6%. After the series of purification procedure, the sugar content of the final product was 97.77%.

3.2. Structural characterization of oyster polysaccharide

3.2.1. Monosaccharide composition

The purified oyster polysaccharide (OG) appeared to be white powder and had no observable absorption at 280 nm and 260 nm, indicating the absence of proteins and nucleic acids. The sulfate content was 0.42%. The "SEC"/size exclusion chromatography profile (Fig. 1A) showed a single, symmetric and sharp peak suggesting that the sample was homogeneous. The average molecular weight was calculated to be 5.8×10^4 g/mol, and the polysaccharide sample was characterized to be merely composed of glucose, by liquid chromatographic analysis of PMP-derivatized samples.

3.2.2. GC–MS analysis of methylation

The fully methylated products were hydrolyzed with acid, converted into alditol acetates, and analyzed by GC–MS. Experimental results showed that the oyster polysaccharide consisted solely of glucose and appeared to have an overwhelming percentage of 1,4,5-tri-*O*-acetyl-2,3,6-tri-*O*-methyl-D-glucitol with some 1,4,5,6-tetra-*O*-acetyl-2,3-di-*O*-methyl-D-glucitol (Table 1). The glycogen nature of the oyster polysaccharide was confirmed because of its typical glycogen linkage characteristics. The ratio of 1,4-linked-glucose to 1,4,6-linked-glucose was 6.6, suggesting that the oyster glycogen chain branches out every 6.6 glucose residues on average. In addition, 2,3,4-Me_3-Glc, 3,6-Me_2-Glc and 2,4,6-Me_3-Glc were also detected, suggesting the existence of trace amount of 1,2,4-linked, 1,6-linked and 1,3-linked glucoses.

3.2.3. NMR analysis

The assigned spectroscopic signals of oyster glycogen are shown in Table 1. The intensive peaks in the ^{1}H and ^{13}C NMR spectra of oyster glycogen were corresponding to the 1,4-D-Glcp residue. The resonances of δ 100.51 ppm (Fig. 2A) were attributed to the anomeric carbon atoms, indicating α anomeric configuration for all monosaccharide residues in OG. There are no carboxyl, acetyl and amido groups in OG because no chemical shift was observed in the region above δ 170 ppm. It was concluded that all sugars were pyran rings since the C-1 resonance bands of furan ring at δ 107 ppm to δ 109 ppm were not observed. The carbon peak at δ 77.65 ppm was indeed C-4 of the 1,4-D-Glcp residue, and it was shifted about 7 ppm downfield compared with the resonance of standard D-Glcp (Agrawal, 1992). The other intensive signals at δ 72.3, 74.1, 71.9, and 61.2 ppm represented C-2, C-3, C-5 and C-6 of 1,4-D-Glcp residue, respectively (de Bruin, Parolis, & Parolis, 1992; Photis & Arthur, 1982; Stevens, Iles, Morris, & Griffiths, 1982). The spectroscopic signals for 1,4,6-D-Glcp and 1-D-Glcp residues were less intensive and some could hardly be observed due to their small amount in the oyster glycogen. Therefore, these observations further confirmed that the oyster polysaccharide was a glycogen, consistent with early report by Motoko, Mariko, and Akira (1996). The structural model of OG was illustrated in Fig. 3.

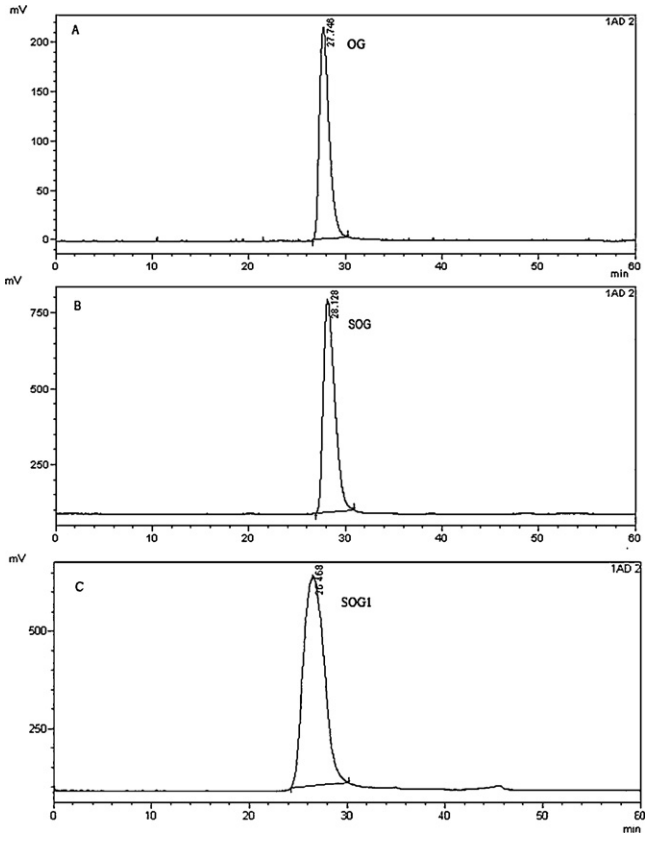

Fig. 1. Size exclusion chromatograms of purified OG (A), SOG (B), and SOG1 (C).

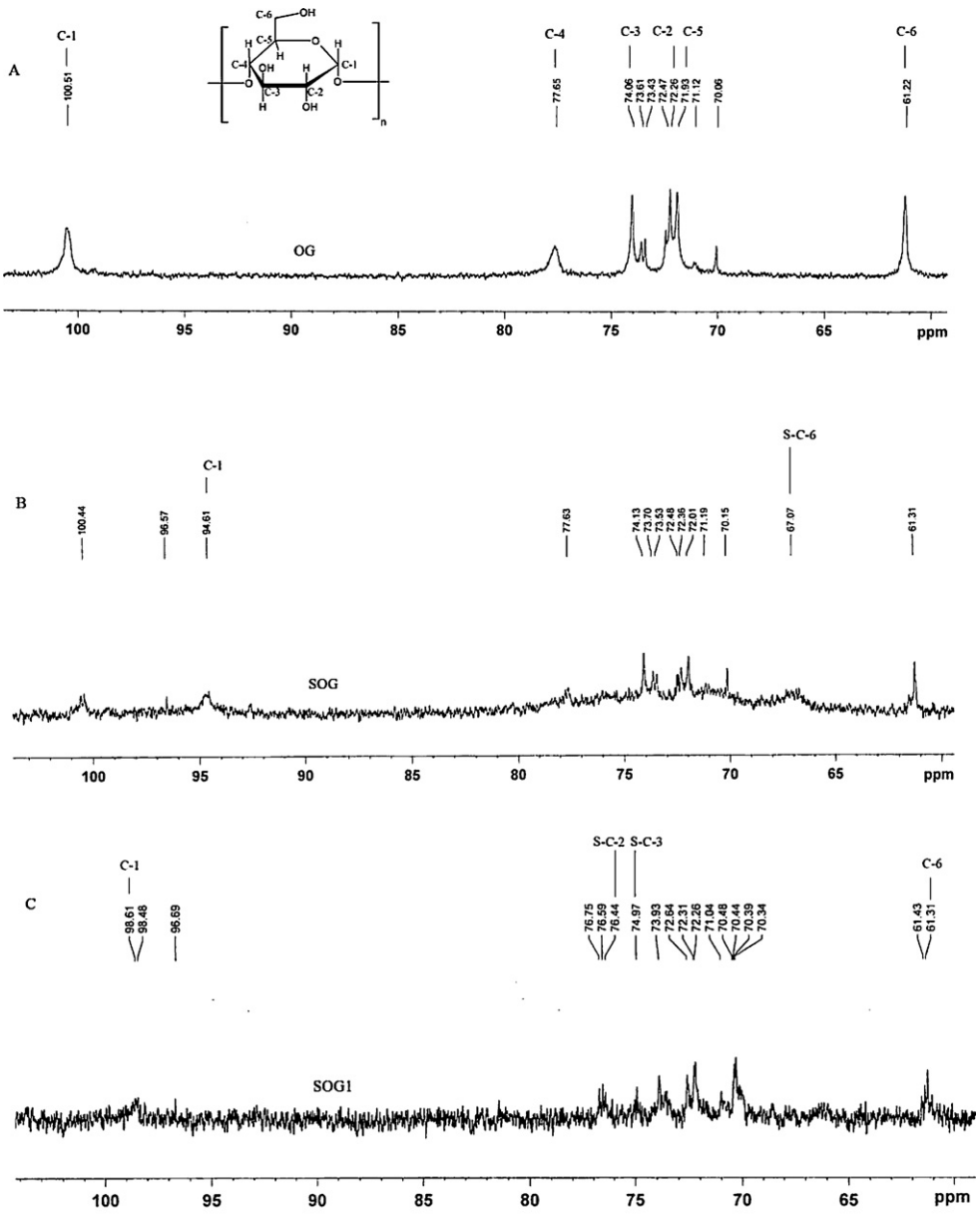

Fig. 2. ^{13}C NMR spectra of OG (A), SOG (B), and SOG1 (C). "S—" indicates the sulfated position.

3.3. Preparation and characterization of sulfated derivatives

3.3.1. Preparation of sulfated oyster glycogen

The oyster glycogen was chemically sulfated with CSA-Pyr method and was further purified by DEAE-cellulose-52 column chromatography. Three fractions of sulfated oyster glycogen were collected, named as SOG, SOG1, SOG2. SOG was the main component. The SOG and SOG1 were well purified as demonstrated by the single and symmetric peak in Fig. 1B and C, respectively. The molecular weights of SOG and SOG1 were determined to be 3.2×10^4 g/mol and 7.9×10^4 g/mol, respectively. The molecular weight of SOG was lower than that of OG. This phenomenon had been observed in variety of sulfated polysaccharides, possibly due to the hydrolysis of side chains under the acidic condition during the sulfation process (Wang, Huang, Wei, Li, & Chen, 2009). The sulfate contents of SOG and SOG1 were measured as 33.6% and 35%, respectively.

3.3.2. IR spectroscopic analysis

The oyster glycogen was analyzed by IR spectroscopy, and the results are shown in Fig. 4. Distinctive absorption peaks of the glycogen were observed: a strong peak at 3400.27 cm^{-1} represents the stretching vibration and angular vibration of O—H linkage; the peaks at 1022.94 cm^{-1} and 1642.64 cm^{-1} represent C—O valence vibration and —O—H deformation vibration, respectively. The peaks at both 2929.30 cm^{-1} and 1383.98 cm^{-1} are caused by stretching vibration and angular vibration of C—H linkage. The characteristic peak at 850.80 cm^{-1} indicates the α-configuration of D-glucan (Barker, Bourne, Stacey, & Whiffen, 1954). Comparing the IR spectrum of SOG with that of OG, as shown in Fig. 4, a distinctive difference could be identified as the band at 1223.05 cm^{-1} emerged which is related to the >S=O stretching. It could be concluded from the above results that sulfate esters were presented in SOG (Lloyd, Dodgson, Price, & Rose, 1961). The strong absorption of SOG at 819.65 cm^{-1} suggested that the sulfate groups were equatorial

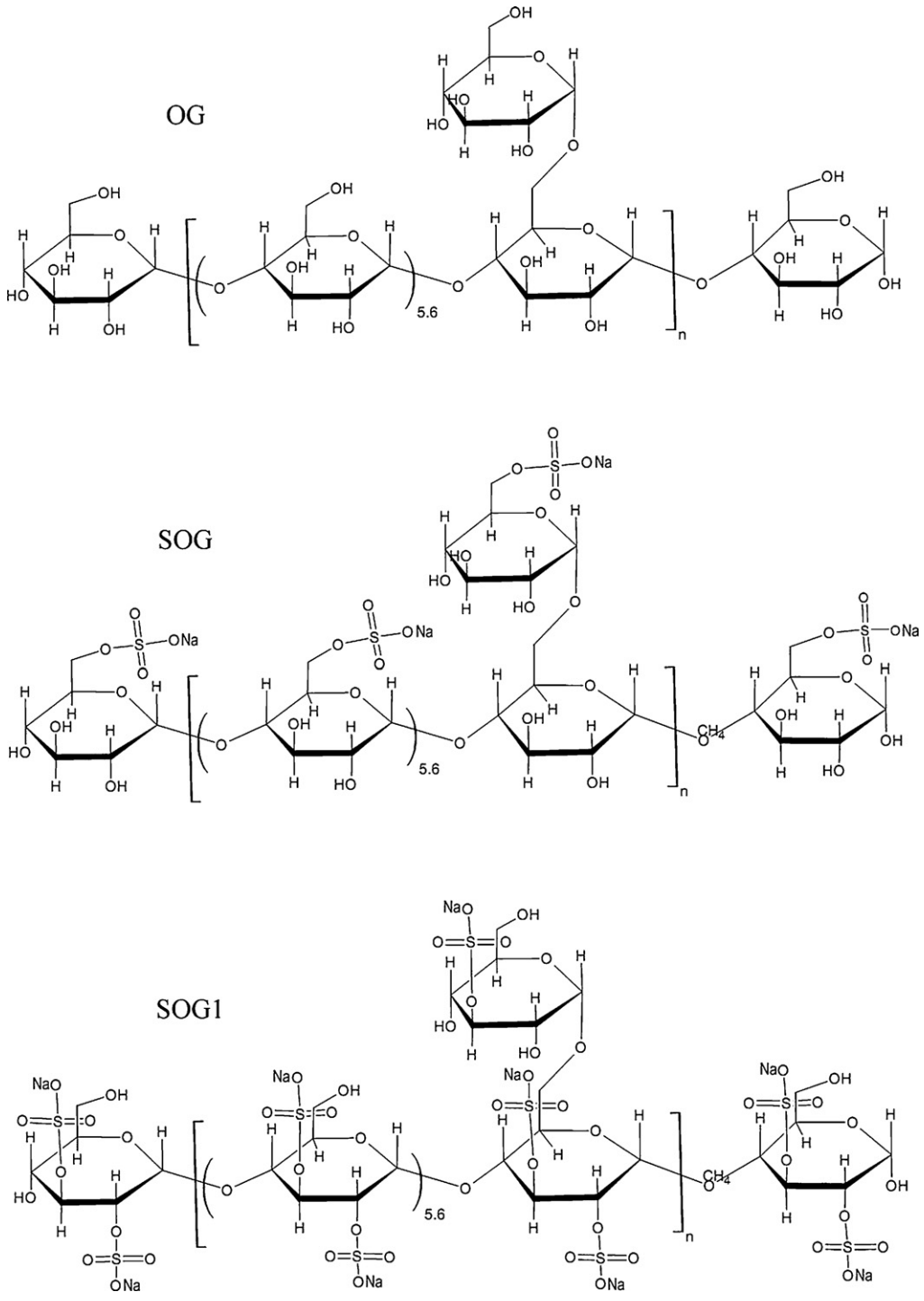

Fig. 3. Structures of oyster glycogen (OG) and two sulfated oyster glycogens (SOG and SOG1).

(Zvyagintseva et al., 2000). A distinctive signature in SOG1 spectrum was observed at band 858.44 cm^{-1}, which was affected by the anomeric structure and the position of sulfate substitution. In general, for the α-galactose residues, the band at 819 cm^{-1} indicated the sulfate is equatorial, and the band at 857 cm^{-1} indicated the sulfate is axial (Yang, Du, Huang, Wan, & Wen, 2005). The results shown in Fig. 4 clearly suggested that the sulfate position of SOG1 was different from that of SOG, which may lead to their different bioactivities.

3.3.3. NMR analysis

^{13}C NMR spectroscopy was utilized to characterize the substitution patterns of sulfate group in SOG and SOG1. SOG was the main component in the sulfation products of the oyster glycogen, while SOG1 was a small-amount by-product.

The ^{13}C NMR spectrum of SOG measured at 30 °C was shown in Fig. 2B. When compared to that of OG, a new peak at δ 67.1 ppm emerged. The signal at δ 67.1 ppm was assigned to C-6 of SOG because it was correlated with two protons at around δ 4.42 ppm

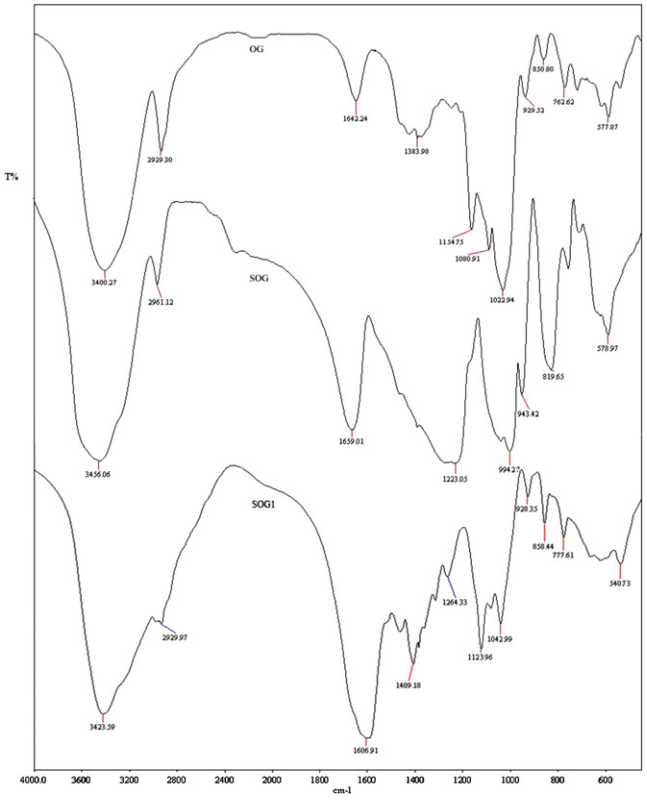

Fig. 4. IR spectra of OG, SOG and SOG1.

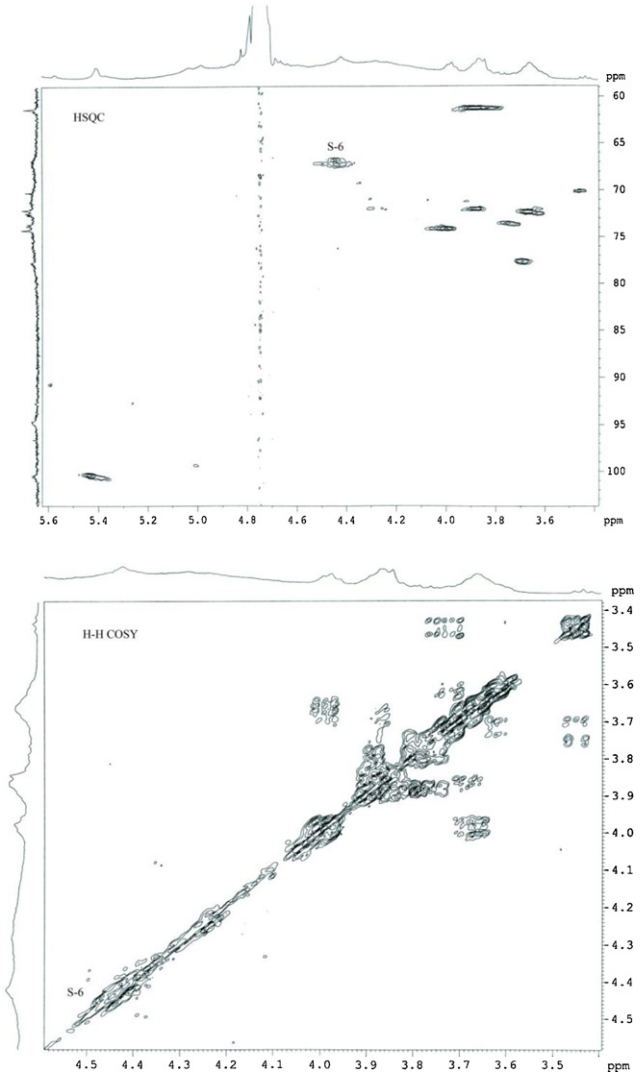

Fig. 5. HSQC and $^{1}H–^{1}H$ COSY spectra of SOG in D_2O. "S-6" indicated the correlations of C-6 with H-6a and H-6b in the HSQC spectrum and the correlation of H-6a with H-6b in the $^{1}H–^{1}H$ COSY spectrum.

in the HSQC spectrum (Fig. 5). And the two protons were identified from their vicinal coupling correlations in the $^{1}H–^{1}H$ COSY spectrum (Fig. 5). Since C-6 was shifted about 6 ppm downfield from the original resonance of δ 61.2 ppm, it was concluded that the sulfate groups were attached to the glucose residues at the C-6 position. The structural model of SOG was illustrated in Fig. 3. The highly branched nature of the oyster glycogen may favor the sulfate substitution at the C-6 position of glucose residues. Furthermore, it has been reported that reactivity of lacquer polysaccharide hydroxyl group was C-6 > C-2 > C-4 (Yang et al., 2005), possibly due to lesser steric hindrance at C-6 positions (Chen et al., 2011). Overall, the sulfate substitution in SOG appeared to be mainly at C-6 positions.

Comparing to that of the OG (Fig. 2C), new peaks at δ 76.44 and 74.97 ppm were observed in the ^{13}C NMR spectrum of SOG1, suggesting sulfate substitution at C-2 and C-3 in SOG1 in agreement with previous reports (Chen et al., 2011; Liu et al., 2009). The peak at around δ 98.61 ppm was assigned to C-1, the resonance change of C-1 was triggered by sulfation at C-2. Therefore, the NMR characterization suggested that the sulfate groups were substituted at C-2 and C-3 in the sulfated SOG1, consistent with the results of IR analysis. The structural model of SOG1 was illustrated in Fig. 3.

3.4. Splenic lymphocyte proliferation activity

The SOG exhibited great splenic lymphocyte proliferation activity *in vitro*, displaying a dose-dependent pattern (Fig. 6). Remarkable activity from SOG was observed at concentrations higher than 20 μg/mL comparing to the normal saline (NS) group ($P < 0.01$), with a 73% increase in lymphocyte proliferation activity at 100 μg/mL SOG comparing to the NS group, and a 66% increase in lymphocyte proliferation activity at 100 μg/mL SOG comparing to the OG group. The results showed that SOG significantly promoted the proliferation of splenic lymphocyte.

Similar stimulation to the proliferation of mice splenic lymphocyte *in vitro* was observed with SOG1 (Fig. 7). The stimulation demonstrated a dose-dependent pattern at concentration of 50 μg/mL and 100 μg/mL. SOG was a stronger stimulator than SOG1, and they were both noticeably more active than normal

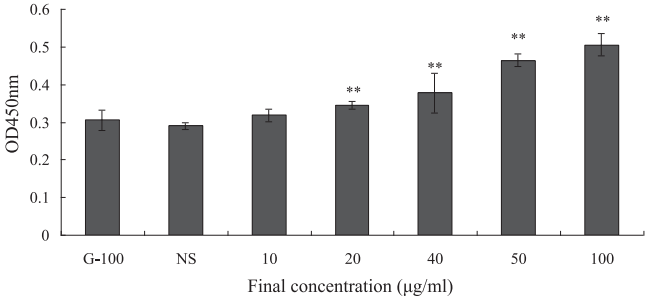

Fig. 6. Stimulation effects of SOG on splenocyte proliferation *in vitro*. G-100, OG at 100 μg/mL; $^{**}P < 0.01$, indicated significant difference vs. normal saline (NS) group.

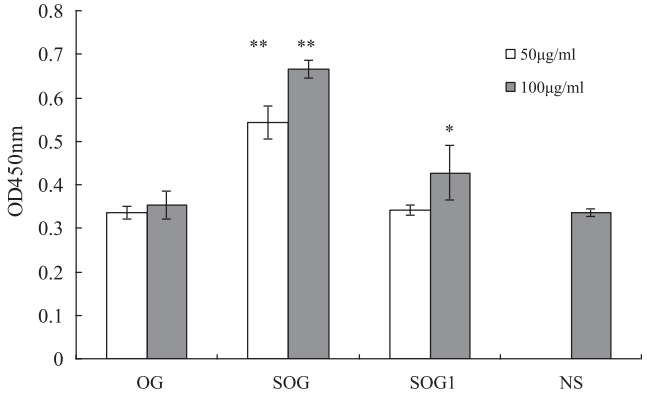

Fig. 7. Stimulation effects of OG, SOG and SOG1 on splenocyte proliferation *in vitro*. $^{**}P < 0.01$, indicated significant difference vs. normal saline (NS) group. $^{*}P < 0.05$, indicated difference vs. normal saline (NS) group.

saline. The OG was much less effective in splenic lymphocyte proliferation stimulation. SOG was a sulfated oyster glycogen with sulfate at C-6 position, yet in SOG1 the sulfate substitution occurred at C-2 and C-3 positions. The sulfate content of SOG and SOG1 were 33.6% and 35%, respectively. The comparison between the structures and activities of SOG and SOG1 indicated that the sulfate substitution position was one of the key structural factors that determines the efficacy of stimulation of the mice splenic lymphocyte proliferation *in vitro*. The sulfate in C-6 position of glycogen appeared to be more effective than sulfate in C-2 and C-3 positions.

Recent studies have reported that some polysaccharides with simple structures could stimulate lymphocyte proliferation. For example, the purified polysaccharide from *Aloe vera* L. var. *chinensis* (Haw.) Berg, mainly composed of β-(1→4)-D-linked mannose with acetylation at the C-6 position of manopyranosyl, exhibited mitogenic activity on murine splenic lymphocytes *in vivo* (Leung et al., 2004). The strong activity of SOG for lymphocyte proliferation *in vitro* might be correlated to its high sulfate content as well as the specific C-6 substitution, which may also play a significant role in the Aloe polysaccharides. The sulfate at the C-6 position of polysaccharide appears to be more effective in promoting splenic lymphocytes proliferation.

4. Conclusion

Purified oyster glycogen was characterized to be α-(1→4)-D-linked glucose that branched every 6.6 residues on average. The sulfated oyster glycogen SOG has a molecular weight of 3.2×10^4 g/mol with sulfate at residues of C-6 positions. The SOG had a simple composition, linkage and sulfate position, and was an excellent model for the study of structure–activity correlation of polysaccharides. High molecular weight and high sulfate content of polysaccharide are essential for the stimulation of lymphocyte proliferation *in vitro*. In addition, products bearing sulfate groups at C6 exhibit better activity than samples that are sulfated at C2 and C3.

Acknowledgments

This work was financially supported by "The National Natural Science Fund" (No. 31171635), "The Projects in the National Science & Technology Pillar Program during the Eleventh Five-year Plan Period" (No. 2008BAD94B07) and "Science & Technology Project of Dalian city" (No. 2011C12CY084).

References

Agrawal, P. K. (1992). NMR spectroscopy in the structural elucidation of oligosaccharides and glycosides. *Phytochemistry*, *31*, 3307–3330.
Barker, S. A., Bourne, E. J., Stacey, M., & Whiffen, D. H. (1954). Infrared spectra of carbohydrates. Part I. Some derivatives of D-glucopyranose. *Journal of the Chemical Society*, 171–176. http://pubs.rsc.org/en/content/articlelanding/1954/JR/jr9540000171#divAbstract
Bradford, M. M. (1976). A rapid and sensitive method for the quantitation of microgram quantities of protein utilizing the principle of protein–dye binding. *Analytical Biochemistry*, *7*, 248–254.
Chen, T., Li, B., Li, Y. Y., Zhao, C. D., Shen, J. M., & Zhang, H. X. (2011). Catalytic synthesis and antitumor activities of sulfated polysaccharide from Gynostemma pentaphyllum Makino. *Carbohydrate Polymers*, *83*, 554–560.
de Bruin, A. H., Parolis, H., & Parolis, L. A. (1992). The capsular antigen of *Escherichia coli* serotype O8:K102:H–. *Carbohydrate Research*, *235*, 199–209.
Dourado, F., Madureira, P., Carvalho, V., Coelho, R., Coimbra, M. A., Vilanova, M., et al. (2004). Purification, structure and immunobiological activity of an arabinan-rich pectic polysaccharide from the cell walls of *Prunus dulcis* seeds. *Carbohydrate Research*, *339*, 2555–2566.
Dubois, M., Gilles, K. A., Hamilton, J. K., Rebers, P. A., & Smith, F. (1956). Colorimetric method for determination of sugars and related substances. *Analytical Chemistry*, *28*, 350–356.
Ghosh, T., Chattopadhyay, K., Marschall, M., Karmakar, P., Mandal, P., & Ray, B. (2009). Focus on antivirally active sulfated polysaccharides: From structure–activity analysis to clinical evaluation. *Glycobiology*, *19*, 2–15.
Leung, M. Y., Liu, C., Zhu, L. F., Hui, Y. Z., Yu, B., & Fung, K. P. (2004). Chemical and biological characterization of a polysaccharide biological response modifier from *Aloe vera* L. var. chinensis (Haw.) Berg. *Glycobiology*, *14*, 501–510.
Liu, Y. H., Liu, C. H., Tan, H. N., Zhao, T., Cao, J. C., & Wang, F. S. (2009). Sulfation of a polysaccharide obtained from *Phellinus ribis* and potential biological activities of the sulfated derivatives. *Carbohydrate Polymers*, *77*, 370–375.
Lloyd, A. G., Dodgson, K. S., Price, R. G., & Rose, F. A. (1961). Infrared studies on sulphate esters. I. Polysaccharide sulphates. *Biochimica et Biophysica Acta*, *46*, 108–115.
Lu, Y., Wang, D. Y., Hu, Y. L., Huang, X. Y., & Wang, J. M. (2008). Sulfated modification of epimedium polysaccharide and effects of the modifiers on cellular infectivity of IBDV. *Carbohydrate Polymers*, *71*, 180–186.
Mosmann, T. (1983). Rapid colorimetric assay for cellular growth and survival: Application to proliferation and cytotoxicity assays. *Journal of Immunological Methods*, *65*, 55–63.
Motoko, M., Mariko, K., & Akira, M. (1996). Fine structural features of oyster glycogen: Mode of multiple branching. *Carbohydrate Polymers*, *31*, 227–235.
Mulloy, B., Mourão, P. A. S., & Gray, E. (2000). Structure function studies of anticoagulant sulphated polysaccharides using NMR. *Journal of Biotechnology*, *77*, 123–135.
Needs, P. W., & Selvendran, R. R. (1993). Avoiding oxidative degradation during sodium hydroxide methyl iodide-mediated carbohydrate methylation in dimethyl sulfoxide. *Carbohydrate Research*, *245*, 1–10.
Photis, D., & Arthur, S. P. (1982). High-field, ^{13}C-NMR spectroscopy of β-D-glucans, amylopectin, and glycogen. *Carbohydrate Research*, *100*, 103–116.
Staub, A. M. (1965). Removal of proteins-Sevag method. Methods in carbohydrate. In *Chemistry*. New York: Academic Press., p. 5.
Stevens, A. N., Iles, R. A., Morris, P. G., & Griffiths, J. R. (1982). Detection of glycogen in a glycogen storage disease by 13C nuclear magnetic resonance. *FEBS Letters*, *150*, 489–493.
Strydom, D. J. J. (1994). Chromatographic separation of 1-phenyl-3-methyl-5-pyrazolone-derivatized neutral, acidic and basic aldoses. *Journal of Chromatography A*, *678*, 17–23.
Sudipta, S., Mojdeh, H. N., Shruti, S., Bandyopadhyay, Paul, S., & Bimalendu, R. (2012). Sulfated polysaccharides from *Laminaria angustata*: Structural features and in vitro antiviral activities. *Carbohydrate Polymers*, *87*, 123–130.
Sun, Y. X., Liang, H. T., Cai, G. Z., Guan, S. W., Tong, H. B., Yang, X. D., et al. (2009). Sulfated modification of the water-soluble polysaccharides from *Polyporus albicans* mycelia and its potential biological activities. *International Journal of Biological Macromolecules*, *44*, 14–17.
Sun, L. M., Zhu, B. W., Li, D. M., Wang, L. S., Dong, X. P., Murata, Y., et al. (2010). Purification and bioactivity of a sulphated polysaccharide conjugate from viscera of abalone *Haliotis discus* hannai Ino. *Food and Agricultural Immunology*, *21*, 15–26.
Therho, T. T., & Hartiala, K. (1971). Method for determination of the sulfate content of glycosamino glycans. *Analytical Biochemistry*, *41*, 471–476.
Wang, L., Huang, H., Wei, Y., Li, X., & Chen, Z. (2009). Characterization and anti-tumor activities of sulfated polysaccharide SRBPS2a obtained from defatted rice bran. *International Journal of Biological Macromolecules*, *45*, 427–431.
Wijesinghe, W. A. J. P., Athukorala, Y., & Jeon, Y. J. (2011). Effect of anticoagulative sulfated polysaccharide purified from enzyme-assistant extract of a brown seaweed *Ecklonia cava* on Wistar rats. *Carbohydrate Polymers*, *86*, 917–921.
Yang, J. H., Du, Y. M., Huang, R. H., Wan, Y. Y., & Wen, Y. (2005). The structure–anticoagulant activity relationships of sulfated lacquer

polysaccharide: Effect of carboxyl group and position of sulfation. *International Journal of Biological Macromolecules*, *36*, 9–15.
Yang, J. F., Zhou, D. Y., & Liang, Z. Y. (2009). A new polysaccharide from leaf of *Ginkgo biloba* L. *Fitoterapia*, *80*, 43–47.
Ye, L. B., Xu, L., & Li, J. R. (2012). Preparation and anticoagulant activity of a fucosylated polysaccharide sulfate from a sea cucumber *Acaudina molpadioidea*. *Carbohydrate Polymers*, *87*, 2052–2057.
Yoshiaki, K., Masahiro, N., Ryoichi, Y., Kaoru, T., Nobuo, S., & Takehiko, K. (1987). Specificity of sulfated polysaccharides to accelerate the inhibition of activated protein C by protein C inhibitor. *Thrombosis Research*, *48*, 179–185.
Zvyagintseva, T. N., Shevchenko, N. M., Nazarova, I. V., Scobun, A. S., Luk'yanov, P. A., & Elyakova, L. A. (2000). Inhibition of complement activation by water-soluble polysaccharides of some far-eastern brown seaweeds. *Comparative Biochemistry and Physiology C: Pharmacology, Toxicology and Endocrinology*, *126*, 209–215.